Polyimide-Functionalized Carbon Nanotubes: Synthesis and Dispersion in Nanocomposite Films

Liangwei Qu,[†] Yi Lin,[†] Darron E. Hill,[†] Bing Zhou,[†] Wei Wang,[†] Xianfeng Sun,[†] Alex Kitaygorodskiy,[†] Myra Suarez,[†] John W. Connell,[‡] Lawrence F. Allard,[§] and Ya-Ping Sun*,[†]

Department of Chemistry, Howard L. Hunter Chemistry Laboratory, Clemson University, Clemson, South Carolina 29634-0973; Advanced Materials and Processing Branch, NASA Langley Research Center, Mail Stop 226, Hampton, Virginia 23681-2199; and High-Temperature Materials Laboratory, Oak Ridge National Laboratory, Oak Ridge, Tennessee 37831-6062

Received May 7, 2004; Revised Manuscript Received June 8, 2004

ABSTRACT: In the preparation of high-quality polymeric carbon nanocomposites, the full compatibility of carbon nanotubes as the filler with the matrix polymer is required. For such a purpose, an amino-terminated polyimide, specifically designed to be structurally identical to the matrix polymer, was synthesized and used in the functionalization of carbon nanotubes. The functionalized carbon nanotube samples were analyzed and studied by using a series of techniques, and the results are presented and discussed. These nanotube samples and the matrix polyimide are soluble in the same organic solvents, allowing their intimate mixing in solution and the subsequent fabrication of polyimide-carbon nanotube composite films via wet-casting. According to results from the spectroscopic and electron microscopic characterizations, the carbon nanotubes are homogeneously dispersed in the nanocomposite films.

Introduction

The use of single-walled (SWNT) and multiple-walled (MWNT) carbon nanotubes in polymeric composites to materialize their superior properties has been attracting much recent attention.[1−6] These nanocomposite materials are explored to attain enhanced mechanical features for efficient load transfer and tear resistance and to achieve certain levels of electric conductivity through a percolation network for charge mitigation and electromagnetic shielding.[1,5−9] However, since carbon nanotubes are generally insoluble and severely bundled, their homogeneous dispersion in desired polymer matrices represents a significant challenge. Several approaches have been proposed and experimented, including the direct suspension of carbon nanotubes in the polymer solution via sonication,[10−15] the in situ polymerization in the presence of carbon nanotubes,[16,17] and the chemical modification of carbon nanotubes for their solubilization.[18−28] For example, several research groups have recently reported the termination of living polymer chains on the carbon nanotube surface or the living polymerization from nanotube-bound initiators, resulting in carbon nanotubes functionalized with polymers of various structures and molecular weights.[24−28]

In the dispersion of carbon nanotubes for high-quality polymeric carbon nanocomposites, an important issue is the selection of dispersion agents such as surfactants in the sonication-based methods and functionalities in the solubilization with chemical modifications. The most desirable way is obviously the use of polymers that are structurally and property-wise identical or close to the matrix polymer in the dispersion or solubilization of carbon nanotubes because it ensures compatibility of the dispersed carbon nanotubes with the polymer matrix to avoid "impurities" associated with the dispersion agents and any potential microscopic phase separation in the nanocomposites.[20,21] For example, Zhu et al. used acid-etched and fluorinated SWNTs in the preparation of epoxy resin-based nanocomposites, where both nanotube-bound carboxylic acids and fluorines could react with the end groups of epoxy resin or the curing reagents under the curing conditions.[22] This was equivalent to the dispersion of epoxy resin-functionalized SWNTs in the matrix of the same resin, and the improved nanotube−matrix compatibility resulted in enhanced composite performance. Sun and co-workers have also shown that polystyrene copolymers with pendant hydroxyl or amine moieties can be covalently attached to carbon nanotubes via the esterification or amidation of the nanotube-bound carboxylic acids and that the soluble functionalized carbon nanotubes can be homogeneously dispersed in polystyrene polymer thin films.[20] More recently, they reported the preparation of poly(vinyl alcohol)−carbon nanocomposite films via solution-casting, in which the carbon nanotubes were functionalized with the matrix polymer for solubility and "impurity-free" dispersion.[21] These nanocomposite films are of high optical quality and exhibit improved mechanical properties.

Aromatic polyimides are candidate polymers for a variety of applications due to their useful properties such as low color, flexibility, high glass transition temperature, excellent thermal stability, and radiation resistance.[29] These polymers serve as excellent matrices for polymeric carbon nanocomposite materials.[8,9,29] Here we report on the homogeneous dispersion of both SWNTs and MWNTs into polyimide matrix for high-quality nanocomposites. The carbon nanotubes were functionalized with a specially synthesized low-molecular-weight polyimide that is structurally identical to the matrix polymer. Results from the characterization of the soluble polyimide-functionalized carbon nanotubes and the fabrication of polyimide−carbon nanocomposite films are presented and discussed.

Experimental Section

Materials. 4,4′-(Hexafluoroisopropylidene)diphthalic anhydride (99%) was purchased from Aldrich, 1,3-bis(3-ami-

[†] Clemson University.
[‡] NASA Langley Research Center.
[§] Oak Ridge National Laboratory.

10.1021/ma0491006 CCC: $27.50
Published on Web 07/17/2004

Scheme 1

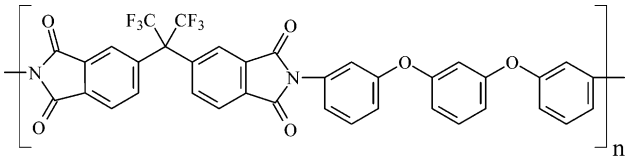

Matrix Polyimide

nophenoxy)benzene was from TCI, 1-ethyl-3-(3-(dimethylamino)-propyl)carbodiimide hydrochloride (EDAC, 98+%) was purchased from Alfa Aesar, and bromobenzene, 4-(dimethylamino)pyridine (DMAP, 99%), and 1-methyl-2-pyrrolidinone (NMP) were from Acros. Toluene, dimethylformamide (DMF), and other solvents were obtained from Mallinckrodt. NMP and DMF were distilled over sodium hydride before use. Deuterated solvents for NMR measurements were supplied by Cambridge Isotope Laboratories. The polyimide based on 4,4′-(hexafluoroisopropylidene)diphthalic anhydride and 1,3-bis-(3-aminophenoxy)benzene (also referred to as LaRC CP-2, Scheme 1) was provided by SRS Inc. ($M_n \sim 17\,100$ and $M_w/M_n \sim 3.2$ according to GPC using polystyrenes as standards).

SWNT and MWNT samples were produced by using the arc-discharge[30] and chemical vapor deposition (CVD) methods,[31] respectively, in Prof. A. M. Rao's laboratory (Physics Department, Clemson University). Both samples were purified via oxidative acid treatment.[20,32] In a typical purification, a nanotube sample (1 g) was suspended in an aqueous HNO_3 solution (2.6 M, 1.5 L) and refluxed for 48 h. Upon vigorous centrifuging, the supernatant was decanted, and the remaining solids were washed repeatedly with deionized water until neutral pH and then dried under vacuum.

Measurements. NMR measurements were performed on a JEOL Eclipse +500 NMR spectrometer. UV/vis/near-IR absorption spectra were recorded on Shimadzu UV3100 and Thermo-Nicolet Nexus 670 FT-NIR spectrometers. Raman spectra were obtained on a Renishaw Raman spectrometer equipped with a 50 mW diode laser source for 785 nm excitation and a CCD detector. Thermogravimetric analysis (TGA) was carried out on a Mettler-Toledo TGA/SDTA851e system. Scanning electron microscopy (SEM) images were obtained on a Hitachi S4700 field-emission SEM system. Transmission electron microscopy (TEM) analyses were conducted on Hitachi HF-2000 TEM and Hitachi HD-2000 TEM/STEM systems, both with the digital imaging capability.

Amine-Terminated Polyimide (PI-NH_2). 1,3-Bis(3-aminophenoxy)benzene (0.512 g, 1.68 mmol) was dissolved in dry NMP (10 mL) in a round-bottom flask. After the solution was cooled in an ice bath for 15 min, 4,4′-(hexafluoroisopropylidene)diphthalic anhydride (0.66 g, 1.47 mmol) was added with vigorous stirring. The ice bath was removed after 1 h, and the reaction mixture was maintained at room temperature for 36 h. After the addition of toluene (4 mL), the flask containing the reaction mixture was attached to a condenser with a toluene-filled Dean−Stark trap and then heated to 150 °C. When the amount of water removed by the azeotrope reached ~0.05 mL, the reaction mixture was cooled to room temperature. Upon the removal of toluene and some NMP on a rotary evaporator, the mixture was precipitated into a large amount of methanol (60 mL). The product as solid precipitate was collected and dried under vacuum at 60 °C (0.98 g, 90% yield). ^{1}H NMR (500 MHz, DMSO-d_6) δ: 8.14 (d, $J = 6.9$ Hz), 7.93 (s), 7.70 (s), 7.57−7.47 (m), 7.47−7.30 (m), 7.27−7.07 (m), 6.98 (t, $J = 7.8$ Hz), 6.94−6.62 (m), 6.33 (d, $J = 8.2$), 6.22 (s), 6.15 ppm (d, $J = 7.8$ Hz).

Nanotube Functionalization. In a typical reaction, EDAC (400 mg, 2.1 mmol) was dissolved in DMF (10 mL). To the solution was added purified SWNTs (51.1 mg), and the mixture was sonicated (VWR Aquasonic 150 HT) for 2 h. To the mixture was added a solution of PI-NH_2 in DMF (100 mg/mL, 5 mL), followed by sonication for another 48 h. The suspension was centrifuged at 3000*g* to separate the dark-colored supernatant from the insoluble residue (unfunctionalized or underfunctionalized nanotubes). Upon solvent removal on a rotatory evaporator, the crude product was redissolved in THF (10 mL) for dialysis in a PVDF membrane tubing (cutoff molecular weight ~250 000) against THF for 3 days. The removal of the solvent THF yielded PI-NH_2-SWNT as a black solid.

The same procedure was applied to the functionalization of MWNTs with PI-NH_2. The PI-NH_2-MWNT sample is also a black solid.

Nanocomposite Films. In a typical experiment, the matrix polyimide (1 g) was dissolved in DMF (2 mL) to form a homogeneous solution. To the solution was added dropwise a DMF solution of PI-NH_2-functionalized carbon nanotubes under constant stirring. The resulting solution was further stirred in a flowing nitrogen atmosphere to slowly evaporate the solvent DMF until the total volume reduced to ~3.5 mL. The viscous solution thus obtained was cast onto a glass substrate with an adjustable film applicator (Gardco). The films were kept in flowing nitrogen atmosphere in a drybox at room temperature for 24 h and then in a vacuum oven at 50 °C for 48 h. The film thickness was measured by using a digital height gage (Nikon Digimicro Stand MS-11C with a MFC-101 digital display device).

Results and Discussion

Polyimide Functionalization of Carbon Nanotubes. The amine-terminated polyimide PI-NH_2 was synthesized by controlling the reaction conditions in the condensation polymerization of 4,4′-(hexafluoroisopropylidene)diphthalic anhydride and 1,3-bis(3-aminophenoxy)benzene. A dianhydride:diamine molar ratio of 7:8 was used for PI-NH_2 with targeted seven repeating units and a molecular weight of ~5200.[33] According to the NMR end group analysis, namely the integrations of the ^{1}H NMR signals for terminal aniline rings at 6.98, 6.33, 6.22, and 6.15 ppm vs those of other aromatic protons, molecular weights of the several batches of PI−NH_2 are in the range 5000−6000, consistent with the synthetic target. FT-IR results of the PI-NH_2 samples exhibit the characteristic imide peaks at 1787, 1730, 1369, and 721 cm^{-1} and phenolic amine peaks at 3510 and 3400 cm^{-1}.[34]

The amine-terminated polyimide PI-NH_2 was used to functionalize SWNTs and MWNTs in carbodiimide-activated amidation reactions with sonication.[4,35] The PI-NH_2-functionalized carbon nanotube samples are soluble in many polar solvents, such as THF, DMF, and DMSO, to form dark-colored homogeneous solutions. Since PI-NH_2 is nearly colorless, the dark solution color serves as a visual indicator for the presence of carbon nanotubes. Shown in Figure 1 is an optical absorption spectrum of the functionalized SWNT sample in DMF solution. The spectrum features absorption bands at 1820 and 1040 nm, corresponding to electronic transitions associated with the van Hove singularities for semiconducting SWNTs (S_{11} and S_{22}, respectively) and a weak band at ~700 nm for metallic SWNTs (M_{11}).[36] These absorption features are typical of SWNT samples produced via the arc-discharge method.[36] Thus, the results seem to suggest that the nanotube electronic structures are largely preserved in the functionalization, consistent with the functionalization being targeted at the defect sites on nanotubes. The solution was also dropped onto a glass slide, followed by the evaporation of DMF, to form a dark-colored transparent thin film. The absorption spectrum of the film shows similarly the characteristic features (Figure 1).

The PI-NH_2-SWNT and PI-NH_2-MWNT samples were characterized by resonance Raman spectroscopy. However, the Raman spectra are subject to strong luminescence interference, similar to those found in other

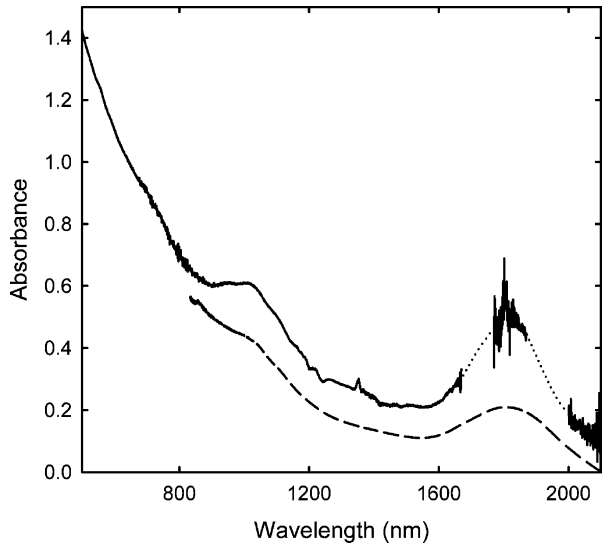

Figure 1. Optical absorption spectra of PI-NH_2-SWNT in DMF solution (—) and as a solid-state sample deposited on a glass substrate (- - -).

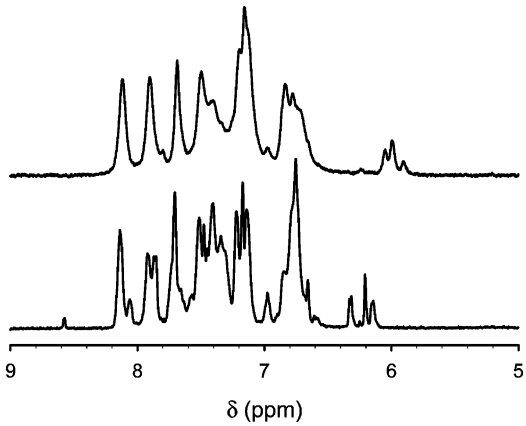

Figure 2. ^{1}H NMR spectra (500 MHz, DMSO-d_6) of PI-NH_2 before (bottom) and after (top) the functionalization with SWNTs.

functionalized carbon nanotubes.[4] After the thermal treatment of these samples at 800 °C in a nitrogen atmosphere to partially remove the functional groups, the luminescence interference becomes less significant. For example, the Raman spectrum of the thermally treated PI-NH_2-SWNT sample shows the characteristic radial breathing mode at 169 cm^{-1}, D-band at 1312 cm^{-1}, G-band at 1590 cm^{-1}, and D*-band at 2566 cm^{-1}.

The solubility of PI-NH_2-functionalized carbon nanotubes enabled high-resolution NMR characterization in solution. Compared in Figure 2 is a comparison of the proton NMR spectra of PI-NH_2-SWNT and PI-NH_2. Both spectra were acquired at the same solution concentration of 3 mg/mL in deuterated DMSO at room temperature. The signal broadening for PI-NH_2-SWNT may be attributed to the attachment of the polyimide to nanotubes as species of high molecular weight and low mobility.[4,20,21,37] In addition to the broadening effect, the nanotube also changes chemical shifts of the protons close to the amide linkages. For the protons of the terminal aniline moiety in PI-NH_2 at 6.4−6.0 ppm, there are upfield shifts of 0.2−0.3 ppm upon the linkage of the polyimide to nanotube (Figure 2).[38]As a result, the three signals move into the 5.9−6.1 ppm region, which is unusual for aromatic protons in substituted benzenes. It is known that the formation of amide linkages results

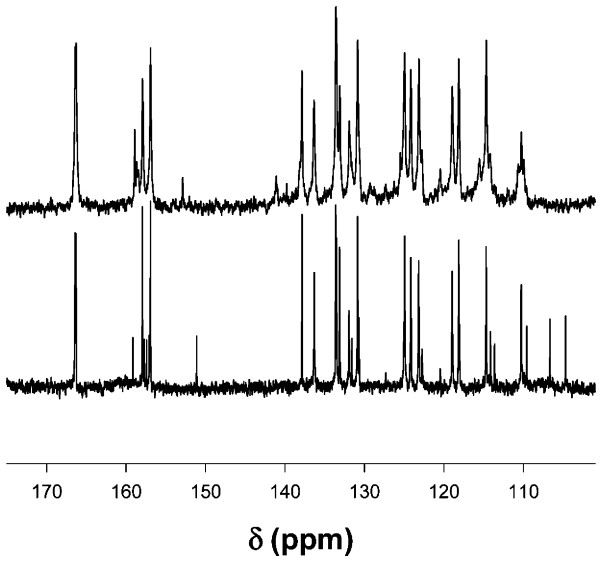

Figure 3. ^{13}C NMR spectra of PI-NH_2 before (bottom) and after (top) the functionalization with SWNTs.

in downfield shifts of the adjacent aromatic protons.[39] At the same time the large aromatic ring currents in carbon nanotubes strongly influence the protons in close proximity to cause upfield shifts in the corresponding NMR signals.[11,15,40,41] Apparently, in this case the competition between the two opposing effects is in favor of net upfield shifts for those protons.

The effects of amide linkages and nanotube ring currents on carbon NMR signals of the terminal aniline units in PI-NH_2 are illustrated in Figure 3. The carbon NMR data also suggest significant changes in chemical environment and/or mobility for terminal aromatic fragments in PI-NH_2 resulting from interactions with the attached nanotubes. The ^{13}C NMR spectra of PI-NH_2 before and after the amidation reaction are mostly similar, with the spectrum after the reaction being somewhat broader. However, the signals at 104.7, 106.8, and 151.0 ppm corresponding to the terminal aniline carbons in free PI-NH_2 are not observed at their original positions in the spectrum of PI-NH_2-SWNT. These signals could be either broadened beyond detection or shifted to other regions where their overlap with more intense signals from repeating aromatic units makes their identification impossible.

The nanotube dispersion in the solubilized samples was examined by TEM. The TEM specimen was prepared by depositing a drop of the sample solution onto a carbon- or holey carbon-coated copper grid, followed by solvent evaporation. As shown in Figure 4, the TEM image of a PI-NH_2-MWNT suggests the presence of amorphous materials on the nanotube surface, which may be attributed to the polyimide functionalities.[42] The functionalized MWNTs of different lengths and diameters are apparently well dispersed in the solubilized sample (Figure 4, inset). The nanotubes appear not significantly shortened despite the amidation reaction condition involving continuous sonication for an extended period of time.[35]

The TEM imaging of functionalized SWNTs is intrinsically more difficult because of the poor contrast between the nanotube and the heavy coating of functional groups. Despite repeated attempts in the TEM analysis of PI-NH_2-SWNT, there was no success to achieve the kind of imaging quality comparable to that for PI-NH_2-MWNT. Instead, a typical TEM image of the

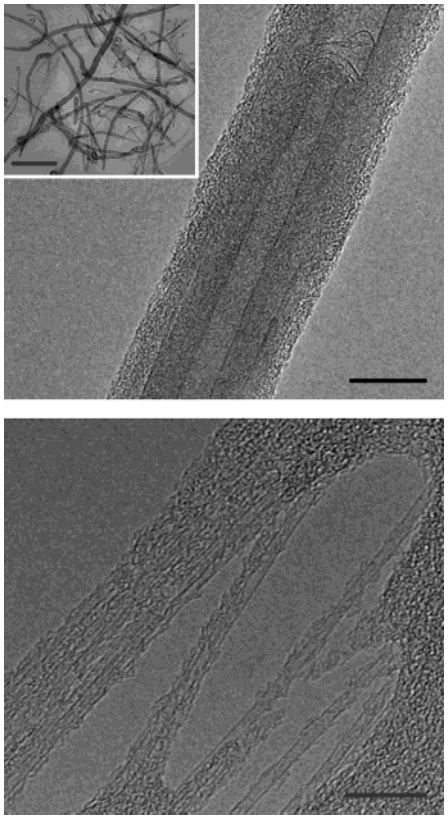

Figure 4. TEM images of the PI-NH_2-MWNT sample at higher (top, scale bar = 15 nm) and lower (inset, scale bar = 200 nm) magnifications and the PI-NH_2-SWNT sample (bottom, scale bar = 10 nm).

PI-NH_2-SWNT specimen shows composite-like structures (Figure 4), with individual or thin bundles of SWNTs covered with amorphous materials. Again, these amorphous materials may be attributed to the polyimide functionalities.[42]

The thermal defunctionalization behavior of the polyimide-functionalized carbon nanotube samples was investigated by TGA. However, because of the thermal stability and unique thermal decomposition pattern of the free polyimide, the thermally selective removal of the functional groups from the nanotube surface has proven to be difficult. In fact, neat PI-NH_2 in a nitrogen atmosphere has a thermal decomposition onset higher than 500 °C, with a substantial amount of residue (close to 60%) remaining at the end of the TGA scan (1000 °C). The TGA trace of PI-NH_2-SWNT is rather similar to that of neat PI-NH_2 (Figure 5), namely that the decomposed polyimide is still associated with the nanotubes in the thermal defunctionalization process. For PI-NH_2 and PI-NH_2-SWNT in air, their TGA traces are also similar. Thus, the polyimide is obviously very different from other polymers such as polystyrene[20] and poly(vinyl alcohol),[21] which could be thermally decomposed and removed to allow the recovery of the nanotubes. Consequently, the TGA estimate of nanotube contents used successfully for many other functionalized carbon nanotubes[4,20,21,43] is not applicable to the polyimide-functionalized samples.

The nanotube contents in the polyimide-functionalized carbon nanotube samples were estimated in terms of quantitative NMR signal integrations in reference to internal standards. Both ^{1}H NMR (4,4′-dimethoxybenzophenone as internal standard) and ^{19}F NMR (trifluoroacetic acid as internal standard) were used, and the

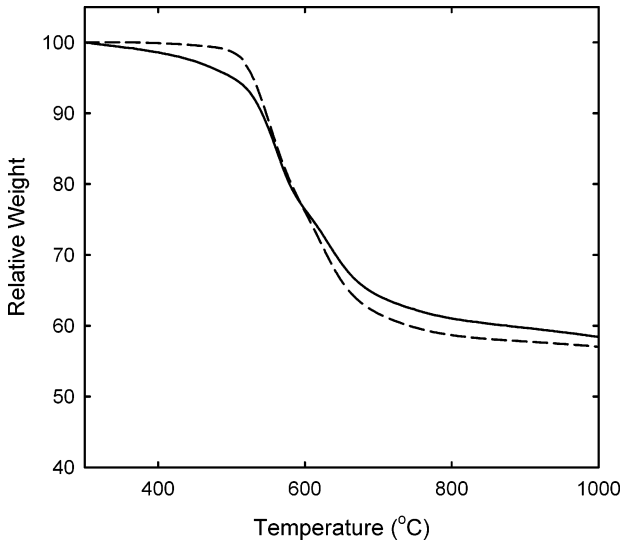

Figure 5. TGA trace of the PI-NH_2-SWNT sample (—) is compared with that of the neat PI-NH_2 sample (- - -).

NMR results (signal integrations of the samples vs those of the internal standards) suggest that the average nanotube contents in the PI-NH_2-SWNT and PI-NH_2-MWNT samples are 15−30% (w/w). In addition, the PI-NH_2-SWNT sample was submitted for elemental analysis, and the fluorine content thus determined is in reasonable agreement with that of the ^{19}F NMR measurement.

The results presented above show that both SWNTs and MWNTs are functionalized by the polyimide to yield functionalized samples soluble in common organic solvents. The solutions of these functionalized carbon nanotubes can be used with a traditional wet-casting method to prepare polyimide−carbon nanocomposites in which the nanotubes are homogeneously dispersed.

Nanocomposite Films. The polyimide based on 4,4′-(hexafluoroisopropylidene) diphthalic anhydride and 1,3-bis(3-aminophenoxy)benzene is a polymer of many desirable properties, such as high optical transparency, thermal stability, solubility in many common solvent systems for solution-phase processing, and especially the durability in the space environment.[8,9,29] As discussed earlier, the PI-NH_2 was designed to be structurally identical to this polyimide and thus fully compatible with the polymer matrix of the nanocomposites. The common solubility of the PI-NH_2-functionalized carbon nanotubes and the matrix polyimide also makes the solution casting easier.

In the film fabrication, the use of carefully dried DMF and the maintenance of a dry environment throughout the experiment are critical because the polyimide films are sensitive to any moisture contamination. The nanocomposite films obtained without moisture contamination in the fabrication appeared optically transparent (even with a dark color in film of a high nanotube loading) and stable under ambient conditions. The films of 25−100 μm in thickness were cut to 1 in. × 3 in. pieces for characterization and other measurements. Shown in Figure 6 is a picture of a series of polyimide−SWNT composite thin films with different nanotube contents.

The optical absorption spectra of the films are similar to those of the solutions with different nanotube concentrations, suggesting that there are no fundamental changes in the PI-NH_2-functionalized carbon nanotubes

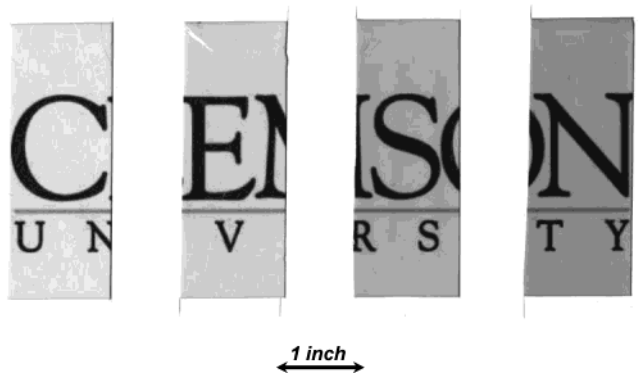

Figure 6. Pictures of four polyimide−SWNT composite films of different nanotube contents (increasing from left to right) over a paper printed with the Clemson logo (to demonstrate that the films are optically transparent).

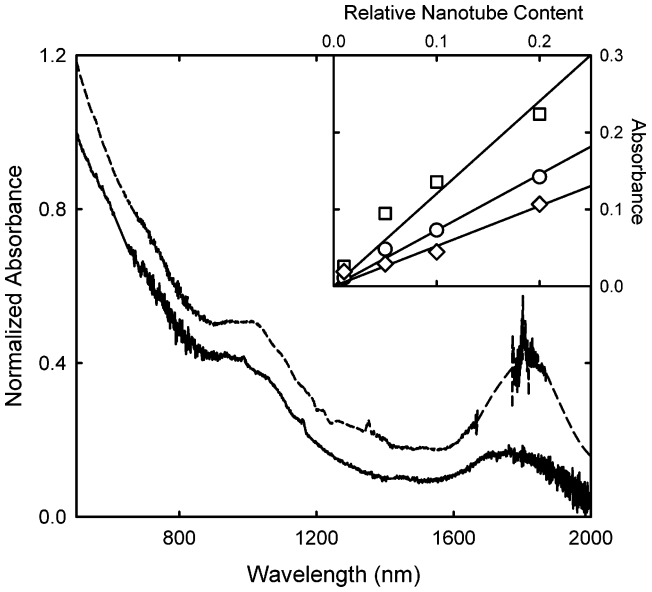

Figure 7. Optical absorption spectrum of a polyimide−SWNT composite film (—) is compared with that of PI-NH_2-SWNT in DMF solution (- - -). Shown in the inset are plots of the absorbance vs the nanotube content from a series of composite films at 500 (□), 1000 (○), and 1800 nm (◇).

upon their dispersion into the polyimide matrix. The spectra of the films are also featured by the characteristic S_{11} and S_{22} absorption bands, with the observed absorbance increases proportional to nanotube contents in the films (Figure 7).

Raman spectra of the polyimide−SWNT composite films, similar to that of the functionalized SWNT sample discussed earlier, contain strong luminescence contributions. The luminescence interference is consistent with the fact that the SWNTs are well dispersed in the polymer matrix.[4,44] After the correction for the luminescence background, the G-band and D-band characteristic of SWNTs can be observed in the Raman spectra.

The dispersion of carbon nanotubes in the polyimide matrix was evaluated more directly by TEM imaging. The specimen were prepared from the microtome of the nanocomposite films in the cross-sectional direction into slices of ~100 nm in thickness. Because of the difficulty with TEM imaging of SWNTs in the presence of polymer matrix, the analysis was concentrated on the polyimide−MWNT composite film. According to the TEM image of the microtomed specimen shown in Figure 8,

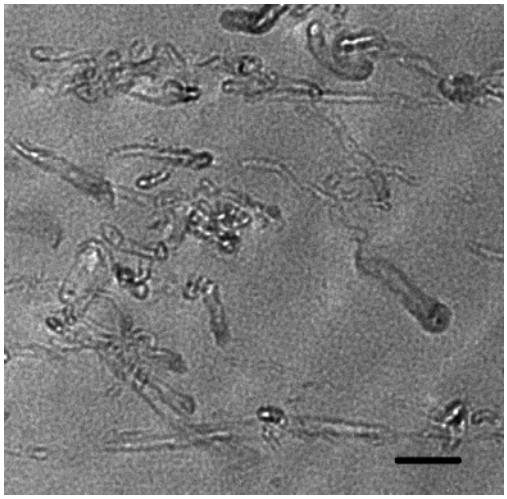

Figure 8. TEM image of the microtomed specimen of a polyimide−MWNT composite film (scale bar = 50 nm).

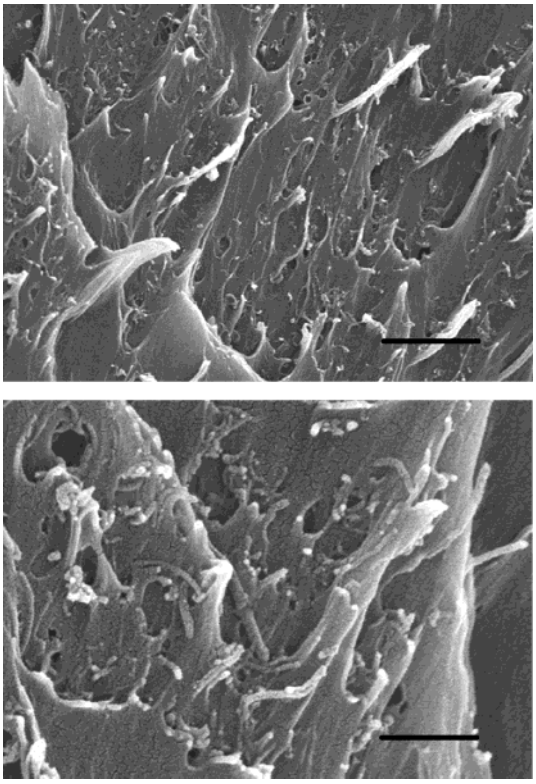

Figure 9. SEM images of the edges resulted from stretching a polyimide−MWNT composite film to failure (top, scale bar = 1000 nm; bottom, a closer look, scale bar = 300 nm).

the MWNTs are apparently well-dispersed at the individual nanotube level in the polyimide matrix.

The same polyimide−MWNT composite film was stretched to failure, and the fractured edges were investigated by SEM. The specimen for the SEM analysis was coated with a thin layer of Pt/Au to minimize surface charging effect. As shown in Figure 9, there are abundant well-dispersed MWNTs protruding out of the polymer matrix near the edge. These protruded nanotubes appear well-wetted by the polyimide, which might be considered as evidence for efficient load transfer between the polymer matrix and filler nanotube in the stretching of the nanocomposite film.[5,45]

In summary, both SWNTs and MWNTs were solubilized by the functionalization with a specifically de-

signed amine-terminated polyimide. The solubilized carbon nanotubes were dispersed into the polyimide matrix via solution-phase mixing and then wet-casting by taking advantage of the common solubility of the functionalized carbon nanotubes and the polyimide in DMF. The design of the amine-terminated polyimide to share the same structural units with the polyimide polymer ensured the full compatibility between the functionalized carbon nanotubes and the polyimide matrix. According to the electron microscopy characterization, the carbon nanotubes are nanoscopically well-dispersed in the polyimide matrix. As a result, the polyimide−carbon nanotube composite films thus obtained are of a high quality, optically transparent, and homogeneous. The reported work demonstrates that a rational design of polymeric functionalities in the solubilization of carbon nanotubes is highly plausible for the fabrication of desirable polymeric carbon nanocomposites.

Acknowledgment. We thank Prof. A. M. Rao for supplying the carbon nanotube samples and S. Fernando for experimental assistance. Financial support from NASA, NSF, and the Center for the Advanced Engineering Fibers and Films (NSF-ERC at Clemson University) is gratefully acknowledged. M.S. was a participant of the Summer Undergraduate Research Program sponsored jointly by NSF and Clemson University. Research at Oak Ridge National Laboratory was sponsored by the Assistant Secretary for Energy Efficiency and Renewable Energy, Office of Transportation Technologies, as part of the HTML User Program, managed by UT-Battelle LLC for DOE (DE-AC05-00OR22725).

References and Notes

(1) Ajayan, P. M. *Chem. Rev.* **1999**, *99*, 1787.
(2) Baughman, R. H.; Zakhidov, A. A.; de Heer, W. A. *Science* **2002**, *297*, 787.
(3) Andrews, R.; Jacques, D.; Qian, D.; Rantell, T. *Acc. Chem. Res.* **2002**, *35*, 1008.
(4) Sun, Y.-P.; Fu, K.; Lin, Y.; Huang, W. *Acc. Chem. Res.* **2002**, *35*, 1096.
(5) Ajayan, P. M.; Stephan, O.; Colliex, C.; Trauth, D. *Science* **1994**, *265*, 1212.
(6) Dalton, A. B.; Collins, S.; Munoz, E.; Razal, J. M.; Ebron, V. H.; Ferraris, J. P.; Coleman, J. N.; Kim, B. G.; Baughman, B. H. *Nature (London)* **2003**, *423*, 703.
(7) Barrau, S.; Demont, P.; Peigney, A.; Laurent, C.; Lacabanne, C. *Macromolecules* **2003**, *36*, 5187.
(8) Park, C.; Ounaies, Z.; Watson, K. A.; Crooks, R. E.; Smith, J. E., Jr.; Lowther, S. E.; Connell, J. W.; Siochi, E. J.; Harrison, J. S.; St. Clair, T. L. *Chem. Phys. Lett.* **2002**, *364*, 303.
(9) Smith, J. G.; Connell, J. W.; Delozier, D. M.; Lillehei, P. T.; Watson, K. A.; Lin, Y.; Zhou, B.; Sun, Y.-P. *Polymer* **2004**, *45*, 825.
(10) Curran, S. A.; Ajayan, P. M.; Blau, W. J.; Carroll, D. L.; Coleman, J. N.; Dalton, A. B.; Davey, A. P.; Drury, A.; McCarthy, B.; Maier, S.; Strevens, A. *Adv. Mater.* **1998**, *10*, 1091.
(11) Star, A.; Stoddart, J. F.; Diehl, M.; Boukai, A.; Wong, E. W.; Yang, X.; Chung, S. W.; Choi, H.; Heath, J. R. *Angew. Chem., Int. Ed.* **2001**, *40*, 1721.
(12) Qian, D.; Dickey, E. C.; Andrews, R.; Rantell, T. *Appl. Phys. Lett.* **2000**, *76*, 2868.
(13) O'Connell, M. J.; Boul. P.; Ericson, L. M.; Huffman, C.; Wang, Y. H.; Haroz, E.; Kuper, C.; Tour, J.; Ausman, K. D.; Smalley, R. E. *Chem. Phys. Lett.* **2001**, *342*, 265.
(14) Star, A.; Steuerman, D. W.; Heath, J. R.; Stoddar, J. F. *Angew. Chem., Int. Ed.* **2002**, *41*, 2508.
(15) Chen, J.; Liu, H.; Weimer, W. A.; Halls, M. D.; Waldeck, D. H.; Walker, G. C. *J. Am. Chem. Soc.* **2002**, *124*, 9034.
(16) Tang, B. Z.; Xu, H. *Macromolecules* **1999**, *32*, 2569.
(17) (a) Cochet, M.; Maser, W. K.; Benito, A. M.; Callejas, M. A.; Martinez, M. T.; Benoit, J.-M.; Schreiber, J.; Chauvet, O. *Chem. Commun.* **2001**, 1450. (b) Barraza, H. J.; Pompeo, F.; O'Rear, E. A.; Resasco, D. E. *Nano Lett.* **2002**, *2*, 797. (c) Shaffer, M. S. P.; Koziol, K. *Chem. Commun.* **2002**, 2074. (d) Kumar, S.; Dang, T. D.; Arnold, F. E.; Bhattacharyya, A. R.; Min, B. G.; Zhang, X.; Vaia, R. A.; Park, C.; Adams, W. W.; Hauge, R. H.; Smalley, R. E.; Ramesh, S.; Willis, P. A. *Macromolecules* **2002**, *35*, 9039.
(18) Mitchell, C. A.; Bahr, J. L.; Arepalli, S.; Tour, J. M.; Krishnamoorti, R. *Macromolecules* **2002**, *35*, 8825.
(19) Grady, B. P.; Pompeo, F.; Shambaugh, R. L.; Resasco, D. E. *J. Phys. Chem. B* **2002**, *106*, 5852.
(20) (a) Hill, D. E.; Lin, Y.; Rao, A. M.; Allard, L. F.; Sun, Y.-P. *Macromolecules* **2002**, *35*, 9466. (b) Hill, D. E.; Lin, Y.; Allard, L. F.; Sun, Y.-P. *Int. J. Nanosci.* **2002**, *1*, 213.
(21) Lin, Y.; Zhou, B.; Fernando, K. A. S.; Liu, P.; Allard, L. F.; Sun, Y.-P. *Macromolecules* **2003**, *36*, 7199.
(22) Zhu, J.; Kim, J. D.; Peng, H.; Margrave, J. L.; Khabashesku, V. N.; Barrera, E. V. *Nano Lett.* **2003**, *3*, 1107.
(23) Wu, W.; Zhang, S.; Li, Y.; Li, J.; Liu, L.; Qin, Y.; Guo, Z.-X.; Dai, L.; Ye, C.; Zhu, D. *Macromolecules* **2003**, *36*, 6286.
(24) Viswanathan, G.; Chakrapani, N.; Yang, H.; Wei, B.; Chung, H.; Cho, K.; Ryu, C. Y.; Ajayan, P. M. *J. Am. Chem. Soc.* **2003**, *125*, 9258.
(25) Yao, Z.; Braidy, N.; Botton, G. A.; Adronov, A. *J. Am. Chem. Soc.* **2003**, *125*, 16015.
(26) Kong, H.; Gao, C.; Yan, D. *J. Am. Chem. Soc.* **2004**, *126*, 412.
(27) (a) Qin, S.; Qin, D.; Ford, W. T.; Resasco, D. E.; Herrera, J. E. *J. Am. Chem. Soc.* **2004**, *126*, 170. (b) Qin, S.; Qin, D.; Ford, W. T.; Resasco, D. E.; Herrera, J. E. *Macromolecules* **2004**, *37*, 752.
(28) Liu, I.-C.; Huang, H.-M.; Chang, C.-Y.; Tsai, H.-C.; Hsu, C.-H.; Tsiang, R. C.-C. *Macromolecules* **2004**, *37*, 283.
(29) Wilson, D.; Stenzenberger, H. D.; Hergenrother, P. M. *Polyimides*; Chapman & Hall: London, 1990.
(30) Journet, C.; Maser, W. K.; Bernier, P.; Loiseau, A.; de la Chapelle, M. L.; Lefrant, S.; Deniard, P.; Lee, R.; Fischer, J. E. *Nature (London)* **1997**, *388*, 756.
(31) (a) Andrews, R.; Jacques, D.; Rao, A. M.; Derbyshire, F.; Qian, D.; Fan, X.; Dickey, E. C.; Chen, J. *Chem. Phys. Lett.* **1999**, *303*, 467. (b) Rao, A. M.; Jacques, D.; Haddon, R. C.; Zhu, W.; Bower, C.; Jin, S. *Appl. Phys. Lett.* **2000**, *76*, 3813.
(32) Hu, H.; Zhao, B.; Itkis, M. E.; Haddon, R. C. *J. Phys. Chem. B* **2003**, *107*, 13838.
(33) Odian, G. *Principles of Polymer Chemistry*, 2nd ed.; Wiley: New York, 1981.
(34) Lee, H.-J.; Lee, M.-H.; Han, S. G.; Kim, H.-Y.; Ahn, J.-H.; Lee, E.-M.; Won, Y. H. *J. Polym. Sci., Part A: Polym. Chem.* **1998**, *36*, 301.
(35) Huang, W.; Lin, Y.; Taylor, S.; Gaillard, J.; Rao, A. M.; Sun, Y.-P. *Nano Lett.* **2002**, *2*, 231.
(36) Hamon, M. A.; Itkis, M. E.; Niyogi, S.; Alvaraez, T.; Kuper, C.; Menon, M.; Haddon, R. C. *J. Am. Chem. Soc.* **2001**, *123*, 11292.
(37) Sun, Y.-P.; Huang, W.; Lin, Y.; Fu, K.; Kitaygorodskiy, A.; Riddle, L. A.; Yu, Y. J.; Carroll, D. L. *Chem. Mater.* **2001**, *13*, 2864.
(38) One of the terminal aniline protons (δ 6.98 ppm before nanotube attachment) could not be unambiguously identified after the functionalization.
(39) Gunther, H. *NMR Spectroscopy*, 2nd ed.; John Wiley & Sons: Chichester, 1995.
(40) Holzinger, M.; Abraham, J.; Whelan, P.; Graupner, R.; Ley, L.; Hennrich, F.; Kappes, M.; Hirsch, A. *J. Am. Chem. Soc.* **2003**, *125*, 8566.
(41) Peng, H.; Alemany, L. B.; Margrave, J. L.; Khabashesku, V. N. *J. Am. Chem. Soc.* **2003**, *125*, 15174.
(42) Lin, Y.; Hill, D. E.; Bentley, J.; Allard, L. F.; Sun, Y.-P. *J. Phys. Chem. B* **2003**, *107*, 10453.
(43) Lin, Y.; Rao, A. M.; Sadanadan, B.; Kenik, E. A.; Sun, Y.-P. *J. Phys. Chem. B* **2002**, *106*, 1294.
(44) Riggs, J. E.; Guo, Z.; Carroll, D. L.; Sun, Y.-P. *J. Am. Chem. Soc.* **2000**, *122*, 5879.
(45) Ajayan, P. M.; Schadler, L. S.; Giannaris, C.; Rubio, A. *Adv. Mater.* **2000**, *12*, 750.

MA0491006